Ω
SPE 36497

Geostatistical Reservoir Modeling Accounting for Precision and Scale of Seismic Data

C.V. Deutsch, SPE, S. Srinivasan, SPE, and Y. Mo, Stanford U.

This paper was prepared for presentation at the 1996 SPE Annual Technical Conference and Exhibition held in Denver, Colorado, U.S.A., 6–9 October 1996.

Abstract

An approach to model the detailed 3-D distribution of lithofacies and porosity constrained to seismic data is presented. The simulated annealing-based approach explicitly honors the relatively coarse vertical resolution, from a reservoir modeling perspective, and the less than perfect correlation of seismic with lithofacies proportions and effective porosity. Conventional geostatistical procedures such as co-located cokriging or the Markov-Bayes model assume that the seismic attribute has the same volumetric support as the geological modeling cells. The conventional techniques are reviewed, details of the proposed methodology are presented, and a reservoir case study is shown.

Introduction

Due to geological complications and inherent limitations in seismic data acquisition, seismic inexactly measures lithofacies proportions and average porosity. Typically, the seismic-derived lithofacies proportion and porosity may be correlated with the true values with a correlation of 0.5 to 0.7. The specific seismic attribute and degree of correlation must be calibrated for each reservoir. Geostatistical techniques to integrate seismic data must account for this precision.

Another consideration, when using seismic data, is that seismic-derived proportions and porosity represent a volume significantly larger than the typical geological modeling cell. The areal resolution is often comparable. The vertical resolution; however, is 10 to 100 times the resolution of the geological modeling cells. Current geostatistical models are built at a vertical resolution of 1-3 feet and current seismic data informs a 30-100 foot vertical average. The detailed resolution of geostatistical models is considered necessary to transfer the effect of heterogeneities into flow simulators.

There is a need for geostatistical modeling tools to explicitly account for the precision and scale of seismic data. Most conventional geostatistical techniques account for the precision of the seismic data by treating it as *soft* or *secondary* data. At times, the seismic data is considered to represent an arithmetic volume average of the lithofacies indicator or the porosity. A review of conventional geostatistical techniques will show that they do not simultaneously handle the precision and scale of seismic data.

An approach will be proposed based on an extension of the simulated-annealing approach to geostatistical model construction. An objective function is constructed that constrains the model to the seismic data accounting for *both* the predefined precision and scale of the seismic data.

An example from a West Texas Permian Basin reservoir is developed to demonstrate the practical applicability of the proposed approach. The 3-D distribution of porosity is constrained to a seismic attribute representing an imprecise ($\rho = 0.5$) 50-foot vertical average.

In an increasing number of cases, seismic data or hand-drawn geological trend maps are available and we want to build them into detailed 3-D geostatistical models. The methodology proposed in this paper is suited to those situations.

The importance of simultaneously accounting for the precision and scale of seismic data could only be assessed by a number of comparative reservoir case studies. These comparative studies are considered important but are not included in this paper. For the time being we must argue that better reservoir models are obtained when they are constrained to the maximum amount of data properly accounting for the precision and scale of each data source.

The Problem

In general, the problem is to build 3-D realizations of lithofacies codes, porosity, and permeability at a sufficiently detailed resolution to provide a reliable basis for well planning, volumetric calculations, and meaningful effective flow properties. We assume that seismic constrains permeability via the lithofacies and porosity, i.e., permeability models will be constructed on a by-lithofacies basis to honor porosity. A collocated assumption is acceptable at that stage since all data relate to the geological modeling cells.

We most often map the lithofacies code, porosity, and permeability at the scale of the data on a network of grid nodes that we call geological modeling cells. That is, we are modeling pseudo-point properties on a grid that is coarse with respect to the point (core/log) data scale. Convenient methods have not been devised to model geological modeling cells accounting for the internal heterogeneities. Some reasons for this difficulty include (1) there would be a mixture of lithofacies in each geological modeling cell, (2) the relationship between porosity and permeability is known at the core scale, and (3) permeability doesn't average with a simple arithmetic or geometric average.

The main distinction between modeling lithofacies codes and porosity is that a greater variety of methods are typically used to model lithofacies. In particular, object-based schemes and cell-based schemes. A discussion on object-based facies modeling constrained to the scale and precision of seismic-data is presented at the end of the paper. For clarity, we will focus on the modeling of an indicator transform of lithofacies and porosity.

Consider $k=1,\ldots,K$ lithofacies types with the indicator transform at location $\mathbf{u}$, $\mathbf{u}\in A$ (A denotes the area or volume of the reservoir layer under consideration) for type k defined as:

$$i(\mathbf{u};k) = \begin{cases} 1, & \text{if location } \mathbf{u} \text{ in lithofacies } k \\ 0, & \text{otherwise} \end{cases} \quad (1)$$

A volumetric average of a lithofacies indicator over a volume v may be interpreted as the proportion of lithofacies k in v:

$$i_v(\mathbf{u};k) = \int_v i(\mathbf{u};k)dv \quad (2)$$

where $\mathbf{u}$ represents the center of volume v. The indicator transform at a particular location (geological modeling cell) may be 0 or 1. This volumetric average is valued continuously between 0 and 1.

Consider also the porosity $\phi(\mathbf{u})$, $\mathbf{u}\in A$. and the volumetric average of porosity $\phi_v(\mathbf{u})$. The indicator formalism and the Markov-Bayes algorithm in particular consider an indicator coding of the continuous porosity variable:

$$i(\mathbf{u};\phi) = \begin{cases} 1, & \text{if location } \phi(\mathbf{u}) \le \phi \\ 0, & \text{otherwise} \end{cases} \quad (3)$$

The indicator transform at a series of threshold values informs the probability distribution of $\phi(\mathbf{u})$.

The volumetric average properties have less variance than the pseudo-point (or geological modeling cell) properties. The three scales of interest are the pseudo-point (core/log) scale ($\bullet$), the seismic scale (v), and the scale of the reservoir or area of interest (A). The relationship between the variances (also called dispersion variances) is given by Krige's relation[1]:

$$D^2(\bullet, A) = D^2(\bullet, v) + D^2(v, A) \quad (4)$$

where $D^2(\bullet,A)$ is the variance of points within the reservoir (σ^2 from the stationary histogram of core/log data), $D^2(\bullet,v)$ is the variance of points within the seismic scale volume, and $D^2(v,A)$ is the variance of the seismic scale properties and the reservoir.

Another general relation is that the quantity $D^2(v,V)$ is estimated from the variogram:

$$D^2(v, V) = \bar{\gamma}(V, V) - \bar{\gamma}(v, v) \quad (5)$$

where the "gamma bar" values are calculated from the elementary variogram as:

$$\bar{\gamma}(v, v) = \int_v \int_v \gamma(x - y)dxdy \quad (6)$$

where $\bar{\gamma}(\bullet,\bullet)$ is 0.0 since $\gamma(0) = 0$, $\bar{\gamma}(A, A) \equiv \sigma^2$ (the variance) provided that the reservoir A is large with respect to the variogram range. The "gamma bar" values for intermediate volumes v are calculated from the variogram model of the point-support data.

As an example, consider the normal scores transform of porosity. By definition, the variance = $\sigma^2 = \bar{\gamma}(A, A) = 1.0$. The variance of any intermediate volume v is given by $D^2(v, A) = 1.0 - \bar{\gamma}(v, v)$ where $\bar{\gamma}(v, v)$ would be calculated from the variogram model of the core/log data. The variance of seismic-derived porosity may exceed this predicted variance due to the fact that seismic does not directly measure average porosity; there is some imprecision.

These volume-variance relations are well-known in mining geostatistics but less commonly used in petroleum geostatistics.

Interpreting and processing seismic data to obtain the greatest information on lithofacies proportions and porosity is not the subject of this paper. We will assume that we have a seismic attribute (impedance, low frequency, peak amplitude over the interval, some complex non-linear combination from a neural net, etc.) $s_v(\mathbf{u})$ that informs on the proportion of lithofacies k: $i_v(\mathbf{u};k)$ and/or the volumetric average of porosity: $\phi_v(\mathbf{u})$. For convenience, the seismic attribute $s_v(\mathbf{u})$ could be in the units

of the variable of interest (fraction or porosity units).

The nature of the "information" is partially revealed in cross plots between $s_v(\mathbf{u})$ and $i_v(\mathbf{u};k)$ and/or $s_v(\mathbf{u})$ and $\phi_v(\mathbf{u})$ from available well data. An even greater amount of "information" may be revealed by cross plots of the two attributes at different locations, e.g., $s_v(\mathbf{u}+\mathbf{h})$ and $i_v(\mathbf{u};k)$ where the lag vector $\mathbf{h}$ is varied within reasonable bounds. In practice, the areal distribution of the seismic data $s_v(\mathbf{u})$ is dense and the cross plot at $\mathbf{h}=0$ is of greatest importance; other $\mathbf{h}$-cross plots are not necessary.

The v subscript reminds us that seismic data represent a vertical average 10-100 times greater than the scale we are modeling. A calibration cross plot between the seismic attribute $s_v(\mathbf{u})$ and the collocated variable of interest $i_v(\mathbf{u};k)$ and/or $\phi_v(\mathbf{u})$ reminds us that this larger scale information is not precise.

Conventional Techniques

A review of conventional techniques will be given to motivate consideration of the simulated annealing-based approach we are proposing.

One approach to account for seismic data is to use a direct transform of the seismic variable to the lithofacies or porosity. For example, a linear regression or neural network trained on the calibration cross plot, e.g., linear regression. These transform approaches will not be discussed in detail since they do not respect geological variability, the scale of the seismic data, and the inherent uncertainty/imprecision of the seismic data. Moreover, the discussion will be restricted to geostatistical *simulation* algorithms versus *estimation* algorithms. In simulation, we are interested in realizations that have appropriate levels of heterogeneity and that honor the data values without any unnatural spatial discontinuities. Estimation techniques for mapping such as kriging or cokriging are not suitable since they provide too-smooth models[2,3].

Consider modeling the 3-D distribution of porosity $\phi(\mathbf{u})$, $\mathbf{u}\in A$. (not the vertical average $\phi_v(\mathbf{u})$). With the exception of the Gaussian-based techniques, all of the methods could be extended to consider the a categorical lithofacies indicator variable $i(\mathbf{u};k)$.

When necessary, the seismic attribute $s_v(\mathbf{u})$ is replicated for all locations within the seismic data volume $\mathbf{u}\in v$.

External Drift the seismic variable could be used as a trend model for the mean of the porosity[2]. Within the context of stochastic simulation, the local porosity mean is:

$$m_\phi(\mathbf{u}) = a_0 + a_1 s_v(\mathbf{u}) \qquad (7)$$

where a_0 and a_1 linearly rescale the seismic attribute $s_v(\mathbf{u})$; the assumption is that the spatial trends in porosity $\phi(\mathbf{u})$ are informed by a linear rescaling of seismic. In general, this assumption is only valid when there is some functional relationship between the seismic attribute and the variable of interest, e.g., seismic attribute = velocity and variable of interest = depth.

Locally Varying Mean The idea is to transform the seismic attribute to the units of porosity, $s_v(\mathbf{u}) \rightarrow m_\phi^s(\mathbf{u})$, and consider it as a local mean in subsequent simulation of porosity[1,2]. This transformation could use some form of regression or more sophisticated neural networks. Kriging in the stochastic simulation algorithm is then performed with these local averages:

$$\left[\phi(\mathbf{u}) - m_\phi^s(\mathbf{u})\right] = \sum_{\alpha=1}^{n} \lambda_\alpha \left[\phi(\mathbf{u}_\alpha) - m_\phi^s(\mathbf{u}_\alpha)\right] \qquad (8)$$

where $\phi(\mathbf{u})$ is estimated using nearby porosity data, ϕ_α, $\alpha=1,...,n$, the seismic-derived mean values at the location under consideration $m_\phi^s(\mathbf{u})$ and at the data locations $m_\phi^s(\mathbf{u}_\alpha)$, $\alpha=1,...,n$. The kriging weights λ_α, $\alpha=1,...,n$ are derived by the conventional simple kriging equations. Essentially we are working with residuals from the seismic-derived mean properties.

This is an easy-to-apply straightforward approach applicable in cases where a more elaborate calibration approach is considered too time consuming.

Block Kriging Once again, the seismic attribute is transformed to the units of porosity $s_v(\mathbf{u}) \rightarrow m_\phi^s(\mathbf{u})$; however, we make the assumption that $m_\phi^s(\mathbf{u})$ is a direct measurement of the arithmetic average porosity over the volumes v, i.e., we now have data $\phi_v(\mathbf{u}_\beta) = m_\phi^s(\mathbf{u}_\beta)$, $\beta=1,...,N$ where there are N seismic data locations[1,2]. Kriging may then be used with surrounding point porosity data and the seismic-derived block data:

$$\phi(\mathbf{u}) = \sum_{\alpha=1}^{n} \lambda_\alpha \phi(\mathbf{u}_\alpha) + \sum_{\beta=1}^{n'} \lambda'_\beta \phi_v(\mathbf{u}'_\beta) \qquad (9)$$

where the kriging weights λ_α, $\alpha=1,...,n$ and λ'_β, $\beta=1,...,n'$ are obtained from the conventional simple or ordinary block kriging equations. The point-block $\gamma_{\bullet,v}(\mathbf{h})$ and block-block variogram $\gamma_{v,v}(\mathbf{h})$ are given by averaging the porosity or point-point variogram (see previous "gamma-bar" discussion). This approach addresses the scale of the seismic data but does not address the precision; the seismic-derived porosity data are incorrectly considered as perfect block measurements of porosity.

The estimate in equation 7 may be used in either a Gaussian or indicator simulation context; in Gaussian simulation it is the conditional mean, in indicator simulation it is a local probability estimate.

Block Cokriging The same linear estimation scheme (9) could be considered with block cokriging[1,2]. This calls for the calculation and modeling of a point porosity variogram $\gamma_{\bullet,\bullet}(\mathbf{h})$, a point-seismic cross variogram $\gamma_{\bullet,s}(\mathbf{h})$, and a seismic-

seismic variogram $\gamma_{s,s}(\mathbf{h})$. In block kriging (not cokriging) these variograms are analytical functions of the single point porosity variogram $\gamma_{\bullet,\bullet}(\mathbf{h})$. The added flexibility of cokriging demands that they be inferred and fit from the available data. In this way, both the scale and precision can be handled.

This cokriging estimate can be used in either a Gaussian or an indicator simulation context. This full block cokriging estimate is the most rigorous conventional geostatistical approach. It has not caught on in practice (yet) due to the tedious variogram inference, the added computational burden of cokriging, and the added computation required for block kriging. The Markov-Bayes and collocated cokriging alternatives were devised to overcome these limitations.

Markov-Bayes In an indicator simulation context[4,5] (for continuous (3) or categorical variables(2)), the Markov-Bayes algorithm[6] is based on the assumption that the seismic attribute $s_v(\mathbf{u})$ is known at all locations and that it perfectly screens all other seismic data. This Markov assumption allows the cross variogram and variogram of the seismic data to be expressed as simple functions of the point indicator variogram. Recall that the probability estimate:

$$F^*(\mathbf{u};z) = \lambda_0 F(z) + \sum_{\alpha=1}^{n} \lambda_\alpha i(\mathbf{u}_\alpha;z) + \sum_{\beta=1}^{n'} \lambda'_\beta y(\mathbf{u}_\beta;z) \tag{10}$$

where $i(\mathbf{u}_\alpha;z)$, $\alpha = 1,\ldots,n$ are hard indicator data coming from known porosity data and $y(\mathbf{u}_\beta;z)$, $\beta = 1,\ldots,n'$ are soft indicator data coming from a calibration cross plot of porosity and seismic. A cokriging is used to establish the weights $\lambda_\alpha, \alpha = 1,\ldots,n$ and $\lambda'_\beta, \beta = 1,\ldots,n'$. The central idea behind the Markov-Bayes model are relations for the cross i-y and direct y-y variogram based on the direct i-i variogram and calibration coefficients derived from the porosity-seismic cross plot.

Collocated Cokriging assumes that only the collocated seismic attribute $s_v(\mathbf{u})$ needs to be considered. A Markov-type assumption (similar to Markov-Bayes) allows the porosity-seismic cross variogram $\gamma_{\phi,s}(\mathbf{h})$ to be expressed as a simple function of the porosity variogram $\gamma_\phi(\mathbf{h})$; the seismic variogram is not needed since only one seismic data is considered[7,8,9].

The porosity and seismic data are transformed to standard $N(0,1)$ Gaussian distributions y_ϕ and y_s. The estimate is written:

$$y^*_\phi(\mathbf{u}) = \sum_{\alpha=1}^{n} \lambda_\alpha y_\phi(\mathbf{u}_\alpha) + \lambda' y_s(\mathbf{u}) \tag{11}$$

the cross correlogram, $\rho_{\phi,s}(\mathbf{h})$, between y_ϕ and y_s is given by the product of the correlation coefficient of the calibration cross plot and the correlogram of porosity $\rho_\phi(\mathbf{h})$.

Annealing Cosimulation the conventional simulated-annealing procedure considers collocated seismic data together with a correlation coefficient or a full bivariate calibration cross plot. The simulated annealing optimization procedure is then used to arrive at a 3-D model that has the appropriate histogram, variogram, and correlation with seismic. The shortcoming is that the scale of the seismic data is not explicitly honored.

The Proposed Procedure

The simulated annealing procedure has been extensively considered in universities and is being increasingly applied due to its ability to honor a wide variety of input data[10-15]. Simulated annealing is based on an analogy with the physical process of annealing. For 3-D geostatistical modeling, the procedure of simulated annealing may be summarized as:

1. Create an initial 3-D numerical model by randomly assigning the porosity $\phi(\mathbf{u})$ or lithofacies indicator $i(\mathbf{u};k)$ at each grid node. Often, this initial random assignment will be taken from the global histogram.
2. Define an objective function as a measure of difference between desired features and those of the realization, e.g., the objective function could include the squared difference between the variogram that represents the realization and an input variogram derived from data.
3. Perturb the model by assigning a new porosity or lithofacies indicator at a randomly chosen location in the 3-D model.
4. Accept the perturbation when the objective function decreases (or if it increases by an acceptably small amount); reject it if the objective function has increased.
5. The perturbation procedure is continued until a low objective function state is achieved.

The objective function is made up of the weighted sum of components designed to account for different sources of data. The weights are calculated such that all components of the objective function are lowered to zero at the end of the annealing process. Typical components in the objective function are (1) the target histogram, (2) the 3-D variogram, (3) indicator variograms designed to quantify special continuity of extreme low and high values, (4) correlations with collocated secondary data, and (5) well-test derived effective properties.

The idea documented in this paper is to add the correlation between a volumetric average of the variable being mapped and a secondary variable. That is, the correlation between $s_v(\mathbf{u})$ and $i_v(\mathbf{u};k)$ and/or $s_v(\mathbf{u})$ and $\phi_v(\mathbf{u})$ where $i_v(\mathbf{u};k)$ and $\phi_v(\mathbf{u})$ are averages of the lithofacies indicator $i(\mathbf{u};k)$ and the porosity $\phi(\mathbf{u})$ being modeled at a small scale. The seismic attribute $s_v(\mathbf{u})$ is a 2-D grid or, perhaps, a coarse 3-D grid.

A reference correlation coefficient $\rho_{i,s}$ or $\rho_{\phi,s}$ could be established from the calibration well data. The deviation from the model could then be measured by the sum of squared differences between the reference correlation coefficient and that of the model

$$O_c = \left[\rho_{i,s}^{reference} - \rho_{i,s}^{realization}\right]^2 \quad (12)$$

In some cases, we want to reproduce more details from the cross plot relationship between $s_v(\mathbf{u})$ and $i_v(\mathbf{u};k)$ or $s_v(\mathbf{u})$ and $\phi_v(\mathbf{u})$. A discretized bivariate probability distribution could be considered. A series of conditional cumulative distribution functions are denoted:

$$F(\phi_{v,i,j}, s_j) = \text{Prob}\{\phi_v \le \phi_{v,i,j},\ s_j \le s \le s_{j+1}\},$$
$$i = 1,\ldots n_\phi,\ j = 0,\ldots,n_s \quad (13)$$

Where n_ϕ and n_s are the number of average porosity and seismic thresholds respectively, s_j, j=0,...,n_s are the seismic thresholds (s_0=0), and $\phi_{v,i,j}$, $i = 1,\ldots n_\phi$ are the porosity thresholds within seismic class j. The component objective function is written:

$$O_c = \sum_{j}^{n_s} \sum_{i}^{n_\phi} \left[F^{reference}(\phi_{v,i,j}, s_j) - F^{realization}(\phi_{v,i,j}, s_j)\right]^2 \quad (14)$$

Details of the simulated annealing methodology may be found in many places; the central idea is to constrain a volumetric average directly.

Object-Based Lithofacies Modeling

In depositional environments where the genetic geologic units consist of clear geometric bodies, as is the case in many fluvial reservoirs, object-based modeling techniques are used. The iterative scheme proposed above to constrain detailed 3-D realizations to an imprecise vertical average could be used in a straightforward manner. Paper SPE 36514 in this same conference describes a hierarchical object-based scheme that would be appropriate for this purpose. The objective functions given above could be used directly.

Reservoir Example

A location map of the 62 vertical wells from a West Texas Permean Basin reservoir is shown on Fig. 1. The area of interest is 10400 ft by 10400 ft. 3-D seismic data is available over this area. The reservoir layer of interest has a nearly constant thickness of 50 ft. The goal is to create 3-D porosity models that honor the histogram and variogram of porosity in the wells as well as the seismic data. The grid definition for this example is the same in X and Y (65 nodes separated by 160ft.) and 50 units in Z (average cell thickness 1.0 ft.).

Fig. 2 shows the histograms of porosity and the vertical average of porosity.

A number of attributes from the 3-D seismic data were considered to inform the porosity over the layer of interest. Fig. 3 shows the low frequency seismic response. This attribute was selected due to its high correlation with the vertical average of porosity, see Fig. 4. A correlation coefficient of about 0.60 is typical.

The detailed 3-D well-log derived porosity data were transformed to a standard Normal distribution. Experimental variogram values in the vertical, north-south, and east-west directions are shown on Fig. 5. The variogram model fit to these data is shown by the solid line and is given by:

$$\gamma(\mathbf{h}) = 0.0 + 0.6Sph\left(\sqrt{\left(\frac{\mathbf{h}_{vert}}{12}\right)^2 + \left(\frac{\mathbf{h}_{NS}}{3000}\right)^2 + \left(\frac{\mathbf{h}_{EW}}{1000}\right)^2}\right)$$
$$+ 0.4Sph\left(\sqrt{\left(\frac{\mathbf{h}_{vert}}{50}\right)^2 + \left(\frac{\mathbf{h}_{NS}}{30000}\right)^2 + \left(\frac{\mathbf{h}_{EW}}{6000}\right)^2}\right) \quad (15)$$

Using this variogram model (Fig. 5) the $\bar{\gamma}(v,v)$ for v = a 50 foot vertical average is 0.692 (working with a normal score transform). This would imply that the variance of the vertical average data would be 1-0.692=0.308. In units of porosity, the standard deviation of the porosity distribution should decrease from 3.27 to 1.81 ($\sqrt{3.27^2 \bullet 0.308}$). As shown on Fig. 2, the standard deviation of the vertically averaged data is 1.89. The relatively small difference between 1.81 and 1.89 is likely due to the limited number of wells and spatial correlation beyond that implied by the variogram.

The $\bar{\gamma}(v,v)$ value for v = a 160 by 160 by 50 foot geological modeling cell is 0.700 compared to 0.692 for v = a simple 50 foot vertical average. The horizontal variogram has a range large with respect to the size of the geological modeling cells. Correlating the seismic attribute to a vertical average from the wells without considering the horizontal averaging is a reasonable assumption.

The $\bar{\gamma}(v,v)$ value for v = a 160 by 160 by 1 foot geological modeling cell is 0.11 (using the normal scores variogram). This means that the variance of the geological modeling cell volume support decreases by only 11% from the point support data. Admittedly, this depends on how the variogram is modeled for short distance lags; however, the fit on Fig. 5 is quite well informed. Assigning point properties to the relatively large geological modeling cells is a reasonable approximation.

Collocated Cokriging: One of the simplest approaches to account for the seismic data is sequential Gaussian simulation with the collocated cokriging option. The SGSIM program from the second edition of GSLIB was used for this purpose. Fig. 6 shows a horizontal and vertical slice through one SGSIM model. The character of the seismic data, e.g. higher porosity on the NE quadrant, is reproduced. Fig. 7 shows the cross plot reproduction of the vertical average of porosity with the seismic attribute. Note that the correlation (0.9) is significantly greater than the input 0.6 because we are looking at the correlation between the vertical average and not a point-by-point correlation. We did not consider lowering the "point-by-point" correlation to arrive at a vertical average correlation coefficient of 0.6.

Markov-Bayes: Fig. 8 shows slices through a realization generated with an indicator method with the Markov-Bayes model for cokriging (MBSIM program from GSLIB). The B(z) values for the five thresholds were 0.23, 0.33, 0.38, 0.31, and 0.04 for equal probability intervals (porosity thresholds of 6.0, 6.3, 8.0, 9.3, and 10.8%). The realization shows the characteristic "patchy" pattern. Fig. 7 shows the cross plot reproduction of the vertical average of porosity with the seismic attribute. Once again, the correlation is too high.

Proposed Procedure: Applying the proposed simulated annealing algorithm (SASIM in the new GSLIB) leads to the slices shown on Fig. 10 and the cross plot reproduction shown on Fig. 11. The realization looks similar to the Gaussian realization on Fig. 6. and yet the cross plot shows the target correlation of 0.60.

Fig. 12 shows Q-Q plots comparing the distribution of porosity in the 3-D SGSIM, MBSIM, and SASIM models with the input data distribution. All three models reproduce the input data distribution. The departures seen with the MBSIM model are partially due to the lower tail and upper tail extrapolation. The primary reason is that the calibration cross plot is between average porosity and seismic while the model is built and the histogram checked against the 3-D porosity distribution.

Fig. 13 shows the vertical variogram reproduction for the 3 models. The MBSIM and SASIM models closely match the input data-derived variogram model. The Gaussian model reaches a too low sill value because of the large vertical correlation.

As expected, the CPU time of the annealing run is greater than either of the conventional techniques. SGSIM took 1.21 minutes, SISIM (Markov-Bayes option) took 5.02 minutes, and SASIM took 21.1 minutes on a Silicon Graphics POWER Indigo 2.

Conclusions

Integrating seismic attributes in lithofacies or porosity mapping requires both the scale and precision of the seismic data to be taken into account. This paper reviewed conventional geostatistical techniques for integrating seismic data. The conventional techniques do not simultaneously address the issues of scale and precision.

An incremental modification to the simulated annealing-based approach was proposed to explicitly account for the vertical averaging and imprecision of seismic data.

A West Texas reservoir example was developed to illustrate the proposed methodology. The co-located cokriging approach in sequential Gaussian simulation and the Markov-Bayes approach were also demonstrated. The proposed simulated-annealing methodology works as expected. A more complete integration of the seismic data is achieved than conventional techniques.

Some concerns with the simulated-annealing based method (1) the CPU requirements are significantly greater than the conventional techniques (still practical at 21 minutes for a 211250 cell model), and (2) the method requires experience to set the *tuning* parameters to achieve reasonable results.

Nomenclature

$D^2(v,V)$	=	dispersion variance of properties defined over volumes of size v in volumes of size V
$F(z)$	=	cumulative distribution function
γ	=	variogram function
$\mathbf{h}$	=	lag separation vector
i	=	indicator transform data value
λ	=	kriging weight
O_c	=	component objective function
ϕ	=	porosity
ρ	=	correlation coefficient
$\mathbf{u}$	=	location coordinates vector

References

1. Journel, A.G. and Ch. J. Huijbregts, *Mining Geostatistics*, Academic Press, New York, NY, 1978

2. Deutsch, C.V., and Journel, A.G.: *GSLIB: Geostatistical Software Library and User's Guide*, Oxford University Press, New York, NY, 1992.

3. Doyen, P.: "Porosity from Seismic Data: A Geostatistical Approach", Geophysics Vol. 53, No. 10, 1988, pp. 1263-1275.

4. Joseph, C.: *Direct Integration of Seismic-Derived Prior Distributions in the Simulation of a 3-D Petrophysical*

Property, Stanford Center for Reservoir Forecasting (SCRF) Report 9, May, 1996.

5. Doyen, P.M., D.E. Psaila and S. Strandenes: "Bayesian Sequential Indicator Simulation of Channel Sands from 3-D Seismic Data in the Oseberg Field, Norwegian North Sea", SPE Paper 28382 presented at the 69th Annual Technical Conference and Exhibition, Society of Petroleum Engineers, New Orleans, LA, September, 1994, pp. 197-211.
6. Zhu, H.: *Modeling Mixture of Spatial Distributions with Integration of Soft Data*, Ph.D. Thesis, Stanford University, Stanford CA, 1991.
7. Xu, X., T.T. Tran, R.M. Srivastava, A.G. Journel, "Integrating Seismic Data in Reservoir Modeling: the Collocated Cokriging Alternative, SPE paper number 24742 presented at the 67th Annual Technical Conference and Exhibition, Society of Petroleum Engineers, Washington, DC, October, 1992, pp. 833-842.
8. Almeida, A.: *Joint Simulation of Multiple Variables Using a Markov-Type Coregionalization Model*, Ph.D. Thesis, Stanford University, Stanford CA, 1993.
9. Araktingi, U.G., W.M. Bashore, T.T.B. Tran and T.A. Hewett: "Integration of Seismic and Well Log Data in Reservoir Modeling", Reservoir Characterization III, PennWell Publishers, eds: B. Linville and T.E. Burchfield and T.C. Wesson, 1993, pp. 515-554.
10. Kirkpatrick, S., Gelatt, C., Jr., and Vecchi, M., "Optimization by Simulated Annealing," *Science*, Vol. 220, No. 4598, pp. 671-680
11. Farmer, C.L.: "Numerical Rocks," *in* P. King (Ed.), *The Mathematical Generation of Reservoir Geology*: Clarendon Press, Oxford, 1992 (Proceedings of a conference held at Robinson College, Cambridge, 1989).
12. Deutsch, C.V., Annealing Techniques Applied to Reservoir Modeling and the Integration of Geological and Engineering (Well Test) Data: Ph.D. thesis, Stanford University, Stanford, California, 1992.
13. Ouenes, A., Bahralolom, I., Gutjahr, A., and Lee, R.: "Conditioning Permeability Fields by Simulated Annealing," paper presented at the Third European Conference on the Mathematics of Oil Recovery, Delft, Netherlands, June 17-19, 1992.
14. Hird, K.B. and Kelkar, M.: "Conditional Simulation for Reservoir Description Using Spatial and Well Performance Constraints," paper SPE 26418 presented at the 68th Annual Technical Conference and Exhibition of the SPE, Houston, Texas, October 3-6, 1993.
15. Deutsch, C.V. and Cockerham, P.W., "Practical Considerations in the Application of Simulated Annealing to Stochastic Simulation," *Mathematical Geology*, Vol. 26, No. 1, January 1994, pp. 67-82

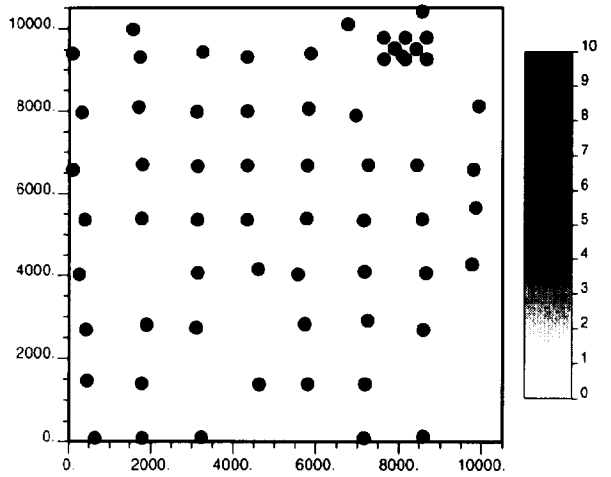

Figure 1: location map of 62 well data. The average porosity is shown by the gray scale level.

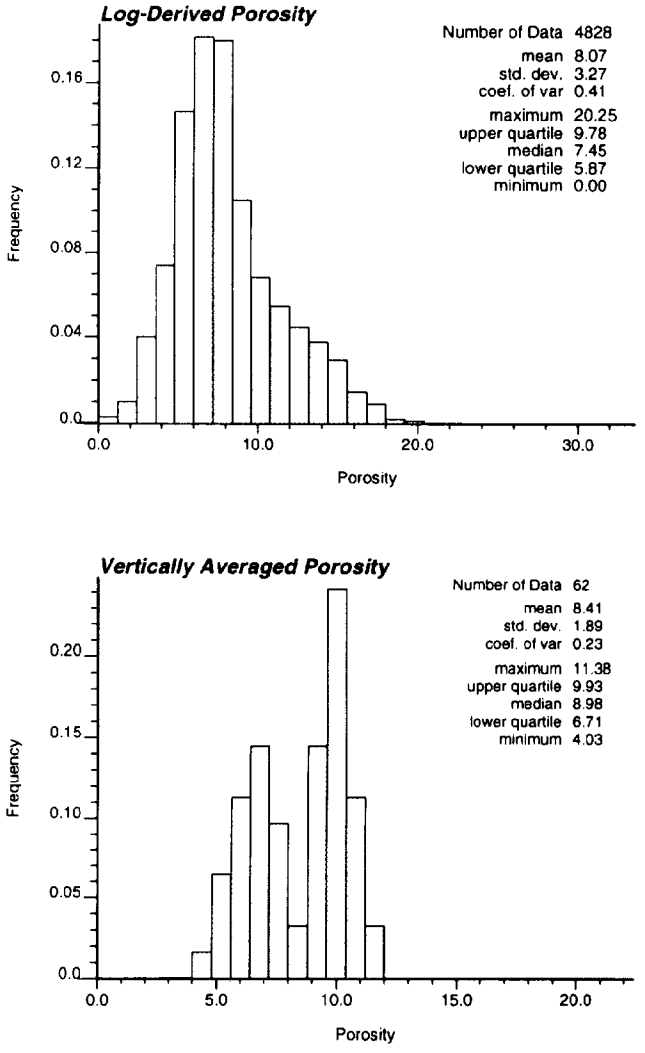

Figure 2: Histograms of the log-derived porosity data and the vertically averaged porosity data.

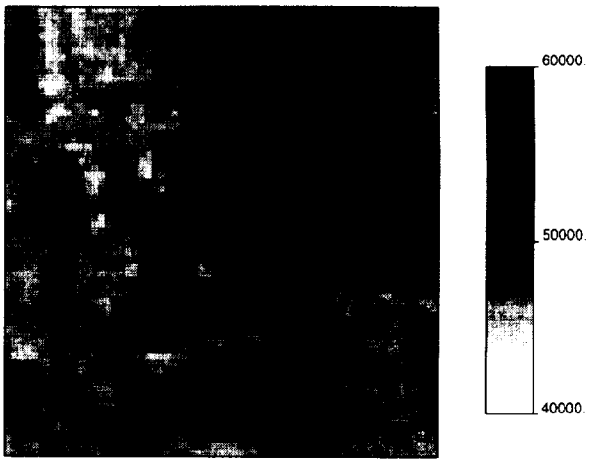

Figure 3: Gray scale map of seismic low frequency attribute over the area of the 3-D seismic survey.

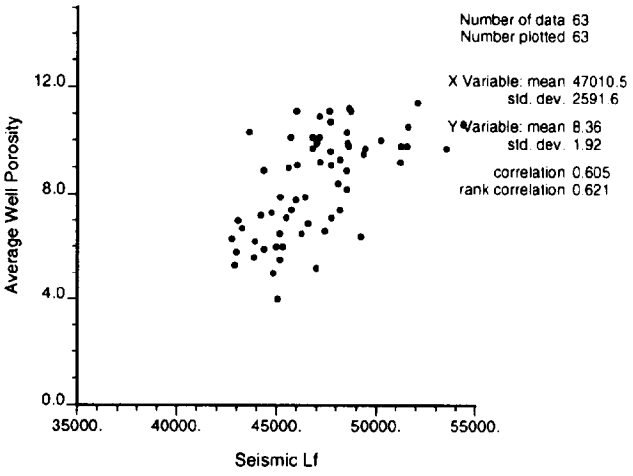

Figure 4: Calibration cross plot between vertical average of porosity and seismic attribute.

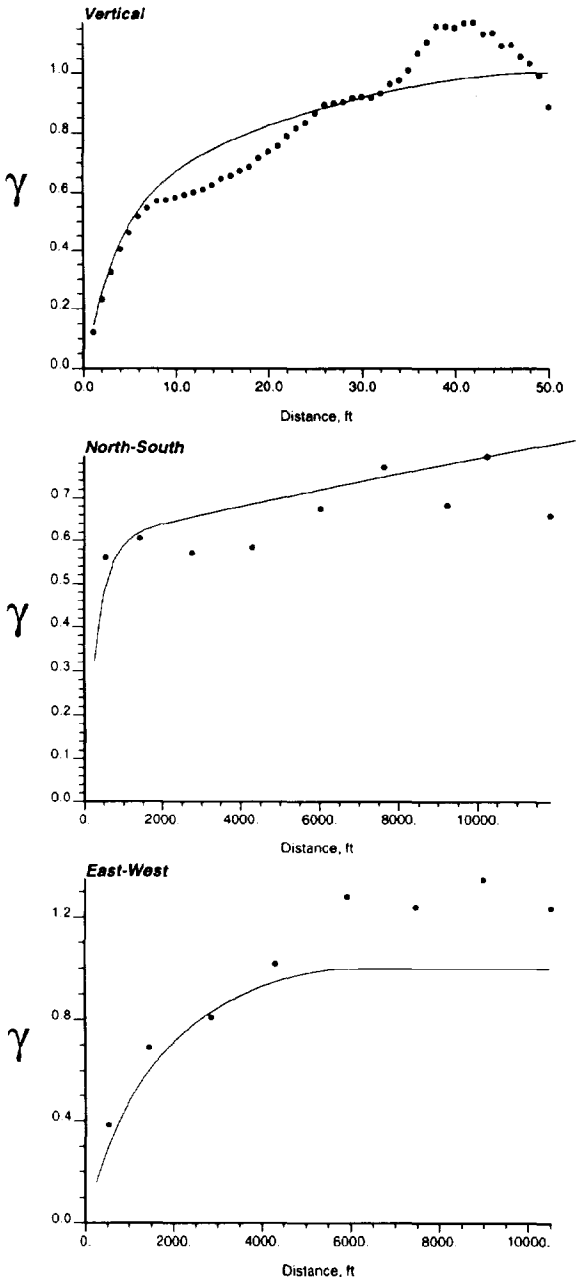

Figure 5: experimental points and 3-D normal scores porosity variogram model.

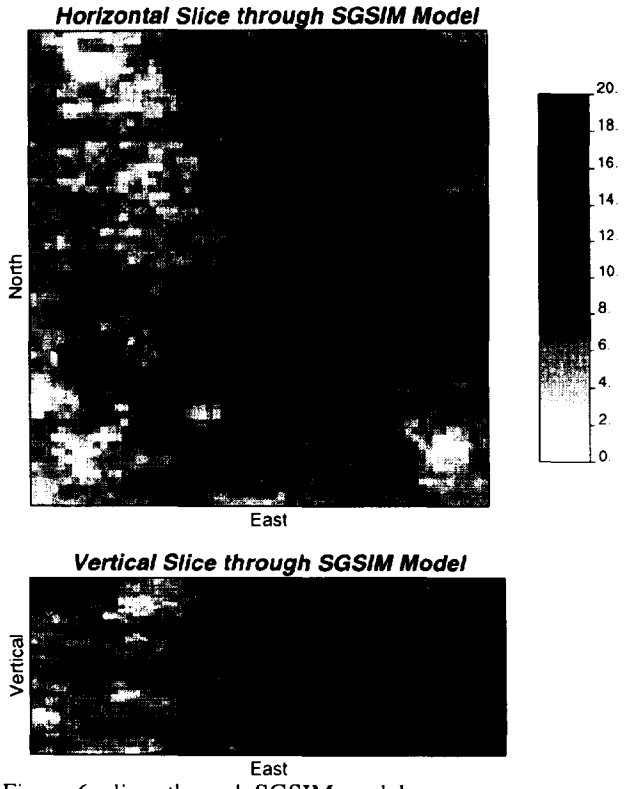

Figure 6: slices through SGSIM model.

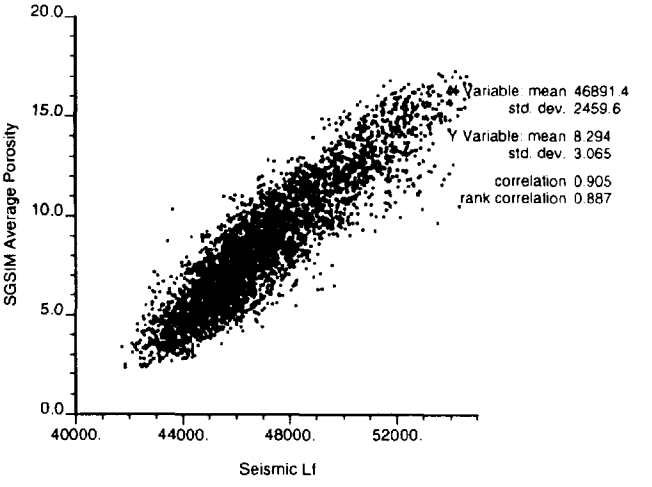

Figure 7: reproduction of cross plot from SGSIM model.

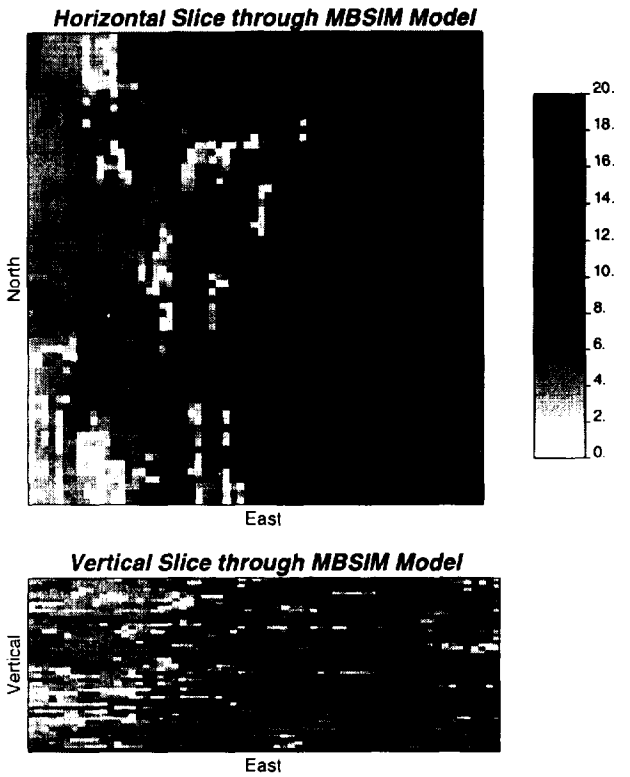

Figure 8: slices through MBSIM model.

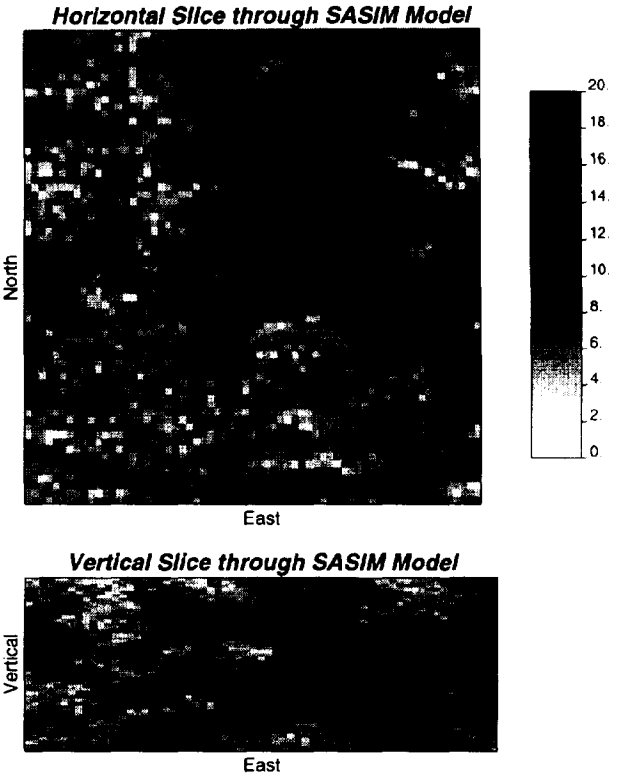

Figure 10: slices through SASIM model.

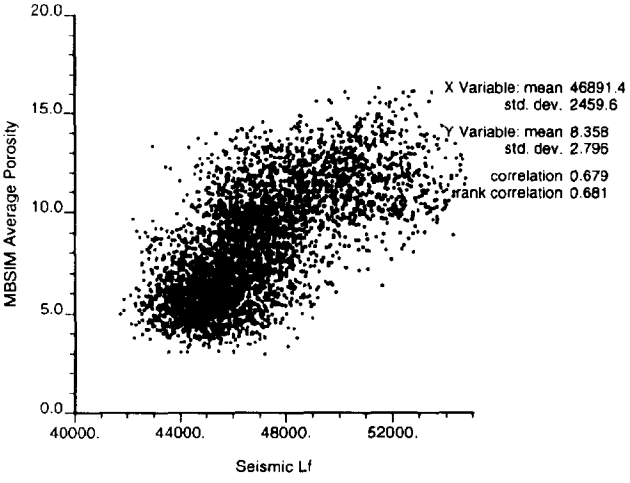

Figure 9: reproduction of cross plot from MBSIM model.

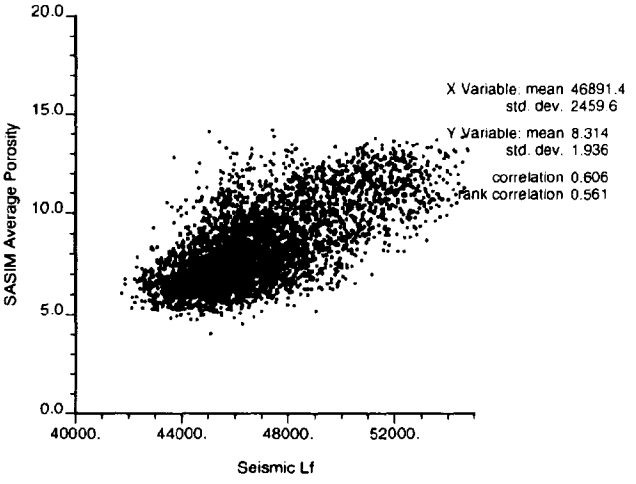

Figure 11: reproduction of cross plot from SASIM model.

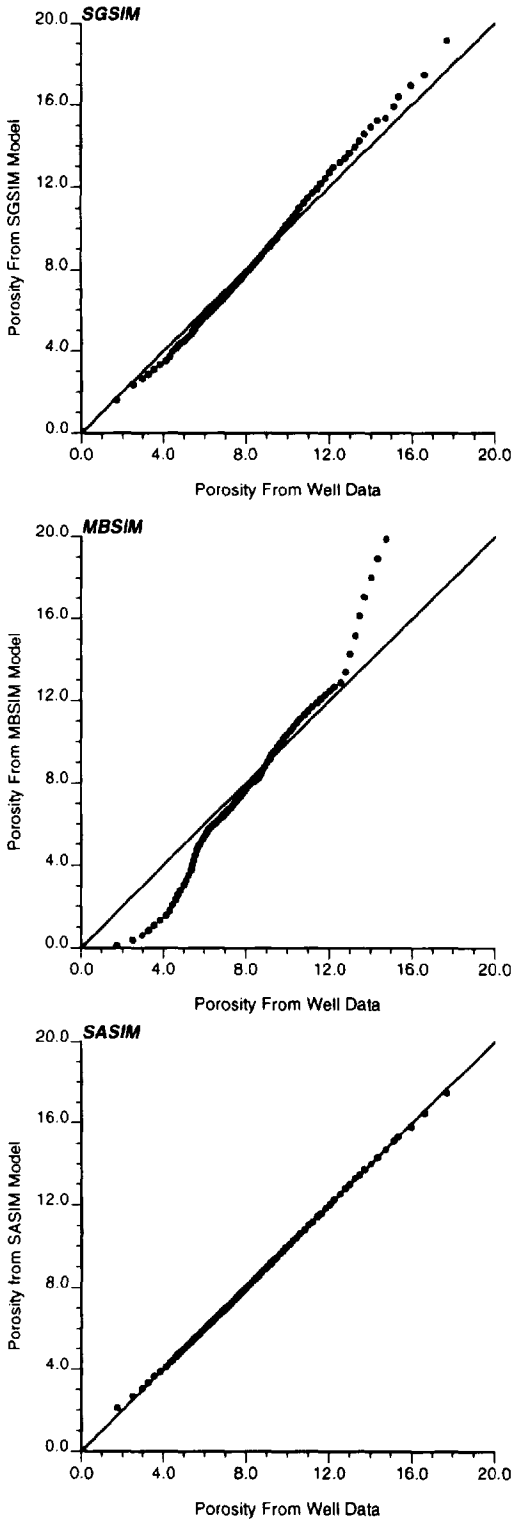

Figure 12: reproduction of porosity histogram by SGSIM, MBSIM, and SASIM models.

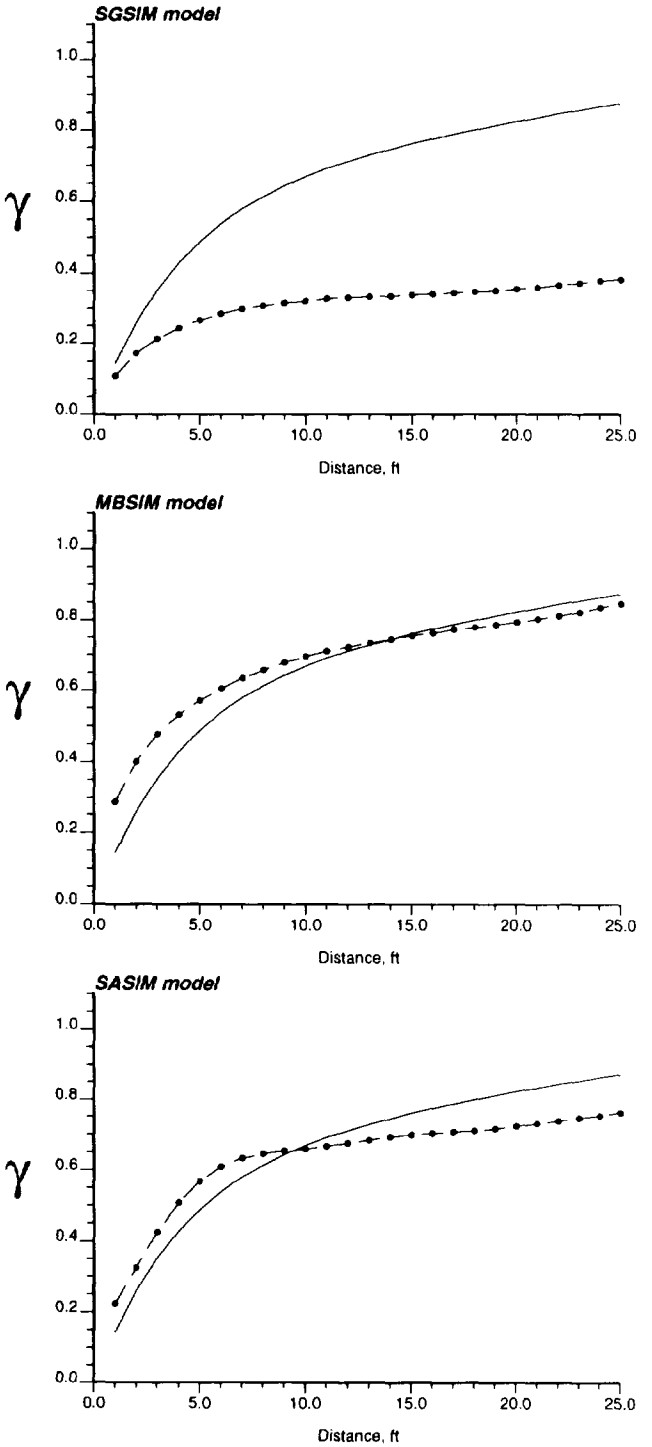

Figure 13: reproduction of vertical variograms by SGSIM, MBSIM, and SASIM models.